

N.V. Mazur¹, A.V. Lysytsya², M.V. Moroz³, B.D. Nechporuk², B.P. Rudyk³,
V.M. Dzhagan^{1,4}, O.A. Kapush¹, M.Ya. Valakh¹, V.O. Yukhymchuk¹

Physical properties of nanocrystalline PbS synthesized by electrolytic method

¹Lashkaryov Institute of Semiconductors Physics, National Academy of Sciences of Ukraine, Kyiv, Ukraine,
kapush-olga@ukr.net

²Rivne State University of Humanities, Rivne, Ukraine

³National University of Water Management and Environmental Management, Rivne, Ukraine

⁴Physics Department, Taras Shevchenko National University of Kyiv, Kyiv, Ukraine

The possibility of obtaining nanocrystalline lead sulfide by an electrolytic method using lead electrodes is demonstrated, and the influence of temperature on the synthesis process is investigated. Based on the results of X-ray diffraction studies, the chemical and phase composition of the obtained samples is determined, as well as the parameters of the unit cell of the crystals lattice. The size of the nanocrystallites and the magnitude of residual mechanical strain in them is determined using the methods of Debye-Scherrer and Williamson-Hall. The results of X-ray diffraction are in agreement with the results of the Raman scattering on phonons.

Keywords: lead sulfide, X-ray diffraction, nanocrystals, Debye-Scherrer formula, Williamson-Hall method, Raman scattering, phonons.

Received 18 November 2022; Accepted 3 April 2023.

Introduction

Lead sulfide (PbS) belongs to narrow-bandgap chalcogenide semiconductors, it has a band gap of 0.41 eV and crystallizes in a cubic crystal system [1]. Due to this, PbS bulk crystals and thin films are widely used in IR detectors, in particular for detecting radiation in the wavelength regions from 1 to 3 μm , which can operate in the temperature range from 77 to 300 K [2]. Due to its unique optoelectronic properties, lead sulfide is also one of the traditional photovoltaic materials [3], and promising for numerous applications in modern optoelectronic devices [3-5], for applications in global positioning systems, software radio systems, environmental monitoring satellites, etc.

In recent years, interest in the development of semiconductor nanostructured materials has been growing rapidly due to their unique physical and chemical properties [6-12]. This is due to their potential application in the field of solar cells of a new generation,

optoelectronic devices, photoconductors, sensors, and infrared detector devices. The attractiveness of PbS nanocrystals stems from the dependence of their properties on size, shape, doping, tunable surface chemistry, and the low cost synthesis. The synthesis of PbS nanocrystals with different morphologies and the corresponding effect on material properties is of great importance in the process of finding new applications in electroluminescent devices, such as light-emitting diodes [7-9]. PbS nanocrystals are especially attractive for devices related to infrared radiation since the energy of their first exciton transition can be easily varied from visible to infrared ranges [7]. Lead sulfide has a large Bohr radius (18 nm) [7], and therefore strong quantization effects can be achieved even for relatively large sizes. The possibility of multiphoton absorption in PbS is extremely useful for the efficiency increase of photoelectronic devices [10]. PbS has a huge potential also in the field of electrochemical biosensors, as well as effective antimicrobial drugs [6, 11].

Semiconductor nanocrystals are obtained by various methods, such as laser sputtering, electrochemical deposition, thermal and magnetron sputtering, mechanical-chemical crushing, chemical deposition, molecular beam epitaxy, synthesis in colloidal solutions, hydrothermal synthesis, electric discharge in water, etc. [12, 13]. In the synthesis of nanomaterials, the choice of research methods is of great importance, especially for controlling dimensional and structural characteristics. It is known that transmission scanning microscopy, optical studies, and X-ray structural analysis are the main methods of studying the dispersion of particles [1,14-17].

I. Experiment and materials

Lead sulfide was obtained by the electrolytic method in an open glass electrolyzer with lead electrodes. A stabilized direct current source was used to power the electrolyzer. Distilled water and the following reagents were used to prepare the electrolyte: sodium thiosulfate ($\text{Na}_2\text{S}_2\text{O}_3 \cdot 5\text{H}_2\text{O}$), sodium chloride (NaCl), and sodium carbonate (Na_2CO_3). Electrolyte concentration was the next: 12.5 g/l in the case of using $\text{Na}_2\text{S}_2\text{O}_3$; 0.625 g/l in the case of NaCl ; 6.25 g/l in the case of Na_2CO_3 . The synthesis process was carried out at the temperature of the electrolyte, which varied from room temperature to 100 C. The duration of the synthesis process was 3 hours, and the current density was 1.3×10^{-2} A/cm². For uniform use of the electrode material, the direct current was reversed after 30 min. After the end of the electrolysis process, the electrolyte was filtered using a paper filter and the resulting powder was washed with five times the volume of distilled water. Samples were air-dried at room temperature.

X-ray studies were carried out on a DRON-4 diffractometer using $\text{CuK}\alpha$ radiation at room temperature. Scanning of XRD pattern was performed according to the Bragg-Brentano scheme (θ - 2θ). The anode voltage and current were 41 kV and 21 mA, respectively. The scanning step of the XRD pattern is 0.05, and the exposure time is 5 s.

For a detailed analysis of experimental XRD patterns, each experimental reflex was described by a Gaussian function, as a result of which the following information was obtained: angular position 2θ , FWHM (full width at half maximum) β , the integrated intensity I . Obtained results were used to interpret experimental XRD patterns and calculate the sizes of nanocrystallites.

Raman light scattering spectra of samples were studied in the backscattering geometry at room temperature. Experimental spectra were recorded using a single-stage spectrometer MDR-23 (LOMO) equipped with a cooled CCD detector (Andor iDus 420, UK). Laser radiation with a wavelength of 457 nm (diode-pumped solid-state laser, CNI Laser) was used as an excitation source for Raman spectra.

II. Results and discussion

Figure 1 shows experimental XRD patterns of samples obtained by the electrolytic method using

different compositions and temperatures of the electrolyte. Using the known interplanar distances and the Wulff-Bragg formula [17,18]:

$$2d \cdot \sin \theta = k \cdot \lambda,$$

where d – interplanar distance; θ – diffraction angle; k – order of the diffraction maximum; λ – wavelength of X-ray radiation, the angular positions of the 2θ reflexes for lead sulfide were calculated. Experimental characteristics of X-ray pattern reflexes (angular position and intensity) were compared with calculations and literature data [6, 17, 19, 20]. It was established that the XRD patterns of the samples shown in Fig. 1 (a) and Fig. 1 (b), contain intense reflexes corresponding to PbS and, accordingly, have the following angular positions 2θ with Miller indices: 26.1 (111); 30.2 (200); 43.2 (220); 51.1; (311); 53.5 (222); 62.7 (400). Thus, using an electrolyte based on $\text{Na}_2\text{S}_2\text{O}_3$ at room and 98 C temperatures allows obtaining lead sulfide without a noticeable content of other compounds.

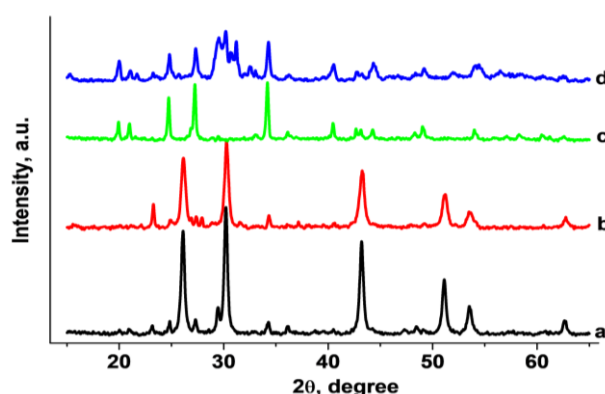


Fig. 1. XRD patterns of samples synthesized by the electrolytic method: a – electrolyte is made using $\text{Na}_2\text{S}_2\text{O}_3$, electrolyte temperature is 98 C; b – electrolyte is made using $\text{Na}_2\text{S}_2\text{O}_3$, the temperature of electrolyte is 23 C; c – electrolyte made using Na_2CO_3 , the electrolyte temperature 20 C; d – electrolyte is made using NaCl , the temperature of the electrolyte is 98 C.

The above XRD patterns (a) and (b) show low-intensity reflexes that do not belong to PbS. It can be assumed that they may refer to lead carbonate and oxide, since we previously showed [21, 22] that when trying to keep cadmium sulfide and zinc oxide by the electrolytic method at room temperature, in addition to these semiconductor nanocrystals, cadmium carbonate and hydrozincite are formed, respectively. Therefore, in this work, two control samples were synthesized - when using an electrolyte based on sodium carbonate and sodium chloride. The XRD patterns of these samples are shown in Fig. 1 (c) and Fig. 1 (d), respectively. A detailed analysis of these patterns showed that there are reflections on them that belong to PbCO_3 and two modifications of lead oxide. Thus, when obtaining lead sulfide by the electrolytic method, carbonate and lead oxide are minor impurities. Carbon dioxide, which is necessary for the lead carbonate formation, is one of the gases dissolved in electrolytes during the electrolysis process since an open electrolyzer is used in our case.

Parameters of the elementary cell are fundamental

values in the identification of crystalline substances, as well as in the determination of chemical bond lengths, the study of transitions from one crystalline phase to another, component composition of solid solutions, and the nature of defects in crystals. The accuracy of determining crystallographic parameters of the sample is affected by several factors, including absorption and refraction of X-rays in the sample, a divergence of the primary beam, dispersion, Lorentz factor and polarization, temperature, etc. [18]. Therefore, it is best to use single crystals to determine the crystallographic parameters of alloys. In the case of nanocrystalline samples, the task is complicated by the large FWHM and low intensity of the peaks in the XRD pattern. In addition, even in the region of large diffraction angles, separation of $K_{\alpha 1,2}$ doublet is not observed. Therefore, we used the extrapolation method to estimate the parameters of elementary cells, since almost all systematic errors of X-ray measurements tend to zero at the diffraction angle $\theta = 90$ [18]. Nanocrystalline PbS obtained in this work, the XRD patterns of which are shown in Fig. 1 (a)-(b), crystallizes in the sphalerite structure, and therefore, using the Wulff-Bragg formula and the quadratic form for cubic crystal system [18], it is possible to calculate the value of unit cell parameter:

$$1/d^2 = (h^2 + k^2 + l^2)/a^2,$$

where a is the crystal lattice parameter; h, k, l are indices of Miller planes.

As an extrapolation function, we used the function [17, 18]

$$f(\theta) = 0.5(\cos^2 \theta / \sin \theta + \cos^2 \theta / \theta).$$

Figure 2 shows the dependence of the unit cell parameter of PbS nanocrystals determined from various reflections on the value of the extrapolation function. A slight deviation of experimental points from linear dependence is visible, and therefore extrapolation line was found by the method of least squares. Calculated values of unit cell parameter are equal to $a = 0.5938$ nm and $a = 0.5935$ nm for samples obtained at electrolyte temperatures of 98 °C and 23 °C, respectively, which is in good agreement with the literature data for single-crystal lead sulfide $a = 0.5936$ nm [20].

The results of processing experimental XRD patterns

were also used to calculate the size of nanocrystals using Debye–Scherrer formula [23]:

$$D = 0.89\lambda/(\beta \cdot \cos \theta),$$

where λ is the wavelength of X-ray radiation; β is the FWHM of the reflex; θ is the diffraction angle. The physical value of the FWHM is calculated by the formula:

$$\beta = (\beta_1^2 - \beta_2^2)^{1/2},$$

where β_1 is the experimental value of the FWHM of the XRD reflex FWHM; β_2 is the instrumental value of the X-ray reflex FWHM. The instrumental value of the X-ray reflexes FWHM was determined based on the analysis of XRD patterns of silicon and Al_2O_3 reference powders, which were obtained under the same conditions.

Using Debye–Scherrer formula, the nanocrystallite size was calculated from all six reflexes and the average value of obtained results was found. As a result, the following sizes of nanocrystals were obtained: 25.9 nm for the sample synthesized at a temperature of 98 °C and 18.8 nm for the case of 23 °C.

The use of Debye–Scherrer formula is based on X-ray reflex FWHM dependence on the particle size, and FWHM increases as size decrease. In addition, it is known that FWHM is affected by mechanical stresses that arise due to defects in a crystal structure. In the case of nanocrystals, defects can appear because a significant part of atoms in them is on the surface, therefore, as the size of nanocrystals decreases, the contribution of surface atoms (surface stress) will increase.

Therefore, to determine the size and mechanical stresses that may be inherent in PbS nanocrystals, we used Williamson-Hall method [24]. In this method, the FWHM of the reflex is described by the following formula:

$$\beta = 0.89 \lambda / (D \cos \theta) + 4 \varepsilon \tan \theta,$$

where λ is the wavelength of X-ray radiation, and ε is the relative elongation. In the last formula, the first term shows contribute to the FWHM is caused by the dimensional effect and the second – by mechanical stresses. We write the last dependence in the form:

$$\beta \cos \theta = 0.89\lambda/D + 4 \varepsilon \sin \theta.$$

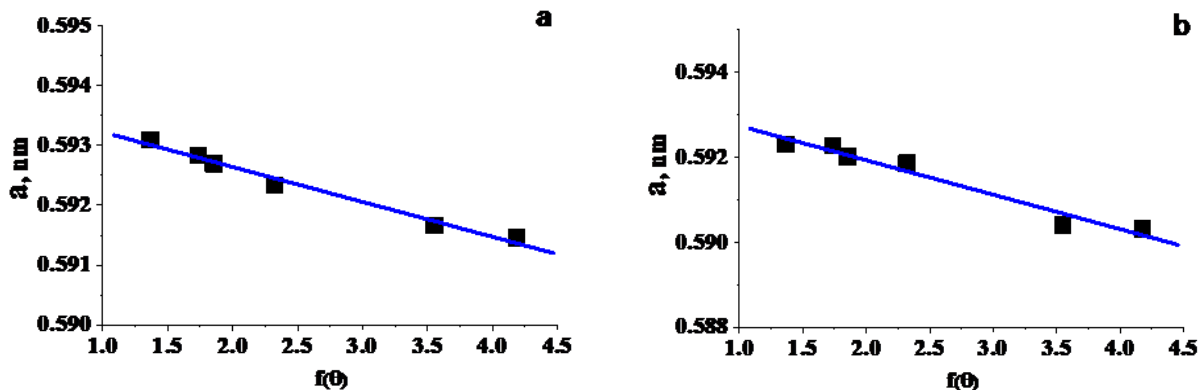


Fig. 2. Graphical extrapolation to determine the crystal lattice parameter of nanocrystalline lead sulfide, obtained at the temperature of the electrolyte: 98 C – a, 23 C – b.

According to Hooke's law, during elastic deformations, the magnitude of mechanical stress is equal to:

$$\sigma = E \cdot \varepsilon,$$

where E is Young's modulus. Having determined the relative elongation from Hooke's law, we obtain the dependence:

$$E^{-1} = s_{11} - (2 s_{11} - 2 s_{12} - s_{44})(h^2 k^2 + k^2 l^2 + l^2 h^2)/(h^2 + k^2 + l^2)^2,$$

where s_{11} , s_{12} , s_{44} are coefficients of elastic compliance. Using the known values of the coefficients of elastic compliance for the cubic modification of lead sulfide $s_{11} = 1.23 \cdot 10^{-12} \text{ Pa}^{-1}$, $s_{12} = -0.33 \cdot 10^{-12} \text{ Pa}^{-1}$, $s_{44} = 4.0 \cdot 10^{-12} \text{ Pa}^{-1}$ [25], as well as the Miller indices of reflections observed on the experimental XRD pattern, we previously calculated the values of Young's moduli depending on the direction inside the single crystal.

Figure 3 shows the use of the Williamson-Hall method to determine the size of nanocrystals and mechanical stresses for two samples. The figure shows the deviation of experimental points from the linear dependence, and therefore the extrapolation line was found by the method of least squares. As a result of using the Williamson-Hall method, the size of PbS nanocrystals was found to be 36.6 nm and the value of mechanical stresses was $1.3 \times 10^8 \text{ Pa}$ (tensile stress) for the samples obtained at a temperature of 98 C, as well as 39.4 nm and $2.5 \times 10^8 \text{ Pa}$ for a temperature of 23 C. The sizes of nanocrystals calculated by Williamson-Hall method are larger than the sizes obtained based on Debye-Scherrer formula. Mechanical tensile stresses for the sample synthesized at a temperature of 23 C are almost two times higher than for the sample obtained at a temperature of 98 C. The latter may indicate that nanocrystals obtained at room temperature have significantly more defects.

Similar results were obtained by the authors of [1], who studied the properties of PbS thin films formed on glass substrates by a chemical method using solutions of lead acetate and thiourea at room temperature. The sizes

$$\beta \cdot \cos \theta = 0.89\lambda/D + 4 \cdot \sigma \cdot \sin \theta/E.$$

If this dependence is plotted in the coordinate system $\langle 4 \sin \theta/E, \beta \cos \theta \rangle$, then we get a straight line from which we can find the nanocrystal size D and the magnitude of mechanical stress σ . For single crystals, Young's modulus will depend on the direction inside the single crystal, that is, on the values of the Miller indices $(h k l)$ and the type of crystal system. This dependence for the cubic system is described by the formula [18]:

of nanoparticles in work [1] were also determined by Debye-Scherrer and Williamson-Hall methods and their values varied from 19 to 23 nm. The authors of the paper [11] studied nanoparticles of lead sulfide obtained by centrifugation of a lead chloride solution and sulfur powder. When the temperature changed from 10 to 40 C, an increase in size from 10 to 25 nm was observed.

Figure 4 represents Raman spectra of two samples of lead sulfide nanocrystals synthesized by the electrolytic method at temperatures of 98 and 23 C, XRD patterns of which are shown in Fig. 1 (a, b), respectively. The figure shows that the spectra of these samples are quite similar. The observed Raman bands were best fitted with a Gaussian function, from which frequency, FWHM, and integral intensity was obtained. The spectra contain two intense scattering bands with a frequency position of 153 and 218 cm^{-1} , as well as bands of low intensity – 88, 191, and 243 cm^{-1} . In addition, the FWHMs are slightly larger at the synthesis temperature of 23 C than at the temperature of 98 C: 11.4 and 10.7 cm^{-1} , respectively, for the band of 88 cm^{-1} , 8.2, and 7.9 cm^{-1} for band 153 cm^{-1} . In the case of a band with a frequency of 218 cm^{-1} , they are the same and equal to 5.2 cm^{-1} .

Bands with frequencies of 88 and 218 cm^{-1} can be attributed to scattering by transverse (TO) and longitudinal (LO) optical phonons at the center of Brillouin zone [26]. The scattering band of LO phonons for PbS is not active in Raman light scattering spectra but is active in IR spectra. It can be manifested in Raman spectra, as noted by the authors of works [27-29], under

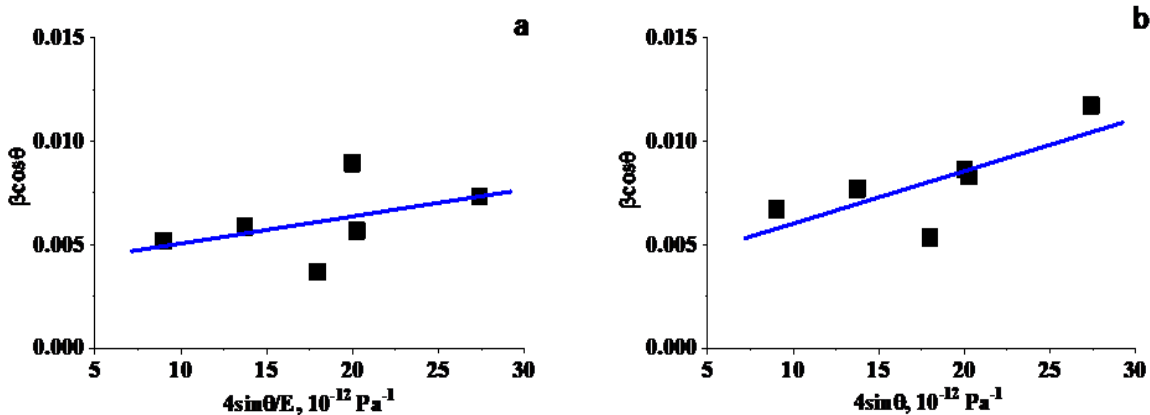


Fig. 3. Results of using Williamson-Hall method for PbS nanocrystals obtained at the temperature of the electrolyte: 98 C – a, 23 C – b.

conditions of resonant or quasi-resonant excitation of Raman spectra due to electron-phonon interaction. In addition, the authors of [30] observed an absorption band at LO phonons (210 cm^{-1}) in the IR spectra. The same opinion on the nature of these scattering bands is held by the authors of works [30, 31].

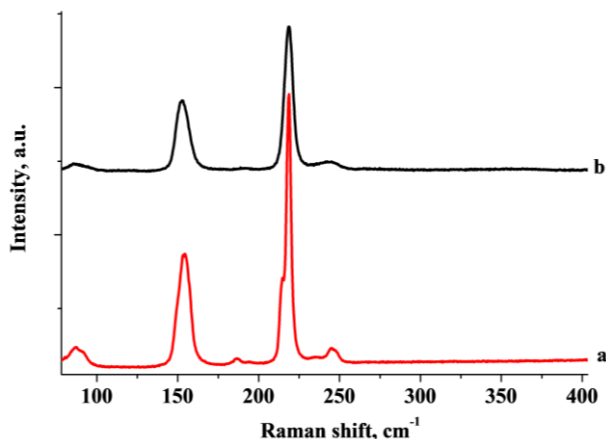


Fig. 4. Raman spectra of samples synthesized using $\text{Na}_2\text{S}_2\text{O}_3$ -based electrolyte at temperatures: a – 98 C; b – 23 C.

In [27], the authors studied Raman spectra of natural PbS and calculated the dispersion curves of lead sulfide for three important directions of Brillouin zone: [100], [111], and [110], as well as the total density of phonon states based on the dispersion curves. They suggested that the band at 190 cm^{-1} is due to the combination of TO + LA phonons along the Δ or Σ direction, and the band at 155 cm^{-1} is due to the combination of TO + TA phonons along the Σ direction. The authors of the work [31] compared Raman spectra of polycrystalline and nanocrystalline PbS and observed a higher value of the scattering frequency for LO phonons in NC, 210 cm^{-1} , compared to a bulk crystal, from 206 cm^{-1} . In our samples, the frequency of the corresponding band is even higher, 218 cm^{-1} , although the size of NC is much larger than in [31], about 20 nm. Therefore, the frequency position of this band in our nanostructures can be determined not by the size effect, but by the dominant contribution of phonons from different dispersion branches of phonons [27].

In [31], thin films of lead sulfide obtained by the chemical method were studied, and scattering bands with frequencies of 148, 192, and 201 cm^{-1} were recorded in Raman spectra. The authors of this paper believe that the band with a frequency of 201 cm^{-1} corresponds to scattering by LO phonons of the center of Brillouin zone, and the band with a frequency of 192 cm^{-1} corresponds to scattering by surface phonons. The nature of the band with a frequency of 148 cm^{-1} is not discussed in [32].

In [33], it is believed that the scattering band of 151 cm^{-1} is due to the combination of TO + TA phonons, and 194 cm^{-1} is due to surface phonons. When studying PbS films in [34], Raman spectra were interpreted as scattering by LO phonons (210 cm^{-1}) and surface phonons

(205 cm^{-1}). An alternative explanation for the origin of the band at 153 cm^{-1} could be the PbO phase [35], but its spectrum is expected to contain a band in the region of $270\text{--}280\text{ cm}^{-1}$, almost equally intense, which is not observed in the spectra of our samples.

For the weak band at 243 cm^{-1} , it is currently impossible to establish the origin. In some works, weak bands in the range of $240\text{--}260\text{ cm}^{-1}$ were also observed, but their nature was not discussed [28].

It is known that PbS nanostructures can undergo significant oxidation, both during synthesis and measurement of Raman spectra since the oxidation is a photostimulated process [36]. However, in the spectra of nanocrystalline PbS obtained in this work by the method of electrolytic synthesis, there are no bands of any of the oxide forms, at least for samples synthesized using an electrolyte based on $\text{Na}_2\text{S}_2\text{O}_3$ (Fig. 4).

Conclusions

This work shows the possibility of synthesizing nanocrystalline lead sulfide by the electrolytic method using lead electrodes and an electrolyte based on sodium thiosulfate. When the temperature of synthesis (electrolyte) increases, the size of PbS nanocrystals increases, and the mechanical tensile stresses acting in the them decrease. The results of Raman scattering spectra are correlated with the results of X-ray structural studies.

Mazur N. – Ph D;

Lysytsya A. – Ph D., Associate Professor of the department of ecology, geography and tourism of Rivne State University of Humanities;

Moroz M. – Dr. Sci, Associate Professor of the Department of Chemistry and Physics of National University of Water Management and Environmental Management;

Nechyporuk B. – Ph D., Associate Professor of the Department of Physics and Astronomy and Teaching Methods of Rivne State University of Humanities;

Rudyk B. – Ph D., Associate Professor of the Department of Chemistry and Physics of National University of Water Management and Environmental Management.

Dzhagan V. - Doctor of Physical and Mathematical Sciences, Professor at Department of Optics and Spectroscopy of Institute of Semiconductor Physics NAS of Ukraine;

Kapush O. – Ph D;

Valakh M. - Doctor of Physical and Mathematical Sciences, Professor at Department of Optics and Spectroscopy of Institute of Semiconductor Physics NAS of Ukraine;

Yukhymchuk V. - Doctor of Physical and Mathematical Sciences, Professor at Department of Optics and Spectroscopy of Institute of Semiconductor Physics NAS of Ukraine.

[1] N. Choudhury and B.K. Sarma, *Structural characterization of lead sulfide thin films by means of X-ray line profile analysis*, Bull. Mater. Sci., 32 (1), 43 (2009); <https://doi.org/10.1007/s12034-009-0007-y>.

- [2] A.B. Rohom, P.U. Londhe, P.R. Jadhav, G.R. Bhand, and N.B. Chaur. *Studies on chemically synthesized PbS thin films for IR detector application*, J. Mater. Sci. 28, 17107 (2017); <https://doi.org/10.1007/s10854-017-7637-4>.
- [3] M.H. Jameel, S. Saleem, M. Hashim, [et al], *A comparative study on characterizations and synthesis of pure lead sulfide (PbS) and Ag-doped PbS for photovoltaic applications*, Nanotechnology Reviews, 10, 1484 (2021); <https://doi.org/10.1515/ntrev-2021-0100>.
- [4] Th. Bielewicz, S. Dogan, and Ch. Klink. Tailoring the Height of Ultrathin PbS Nanosheets and Their Application as Field-Effect Transistors. *Small* 11(7), 826 (2015); <https://doi.org/10.1002/sml.201402144>.
- [5] D.J. Asunskis, I.L. Bolotin, A.T. Wroble, A.M. Zachary, L. Hanley. Lead Sulfide Nanocrystal-Polymer Composites for Optoelectronic Applications. *Macromol. Symp.*, 268, 33 (2008); <https://doi.org/10.1002/masy.200850807>.
- [6] L.F. Koao, F.B. Dejene, H.C. Swart, *Synthesis of PbS Nanostructures by Chemical Bath Deposition Method*, Int. J. Electrochem. Sci., 9, 1747 (2014);
- [7] I. Moreels, K. Lambert, D. Smeets, D. De Muynck, T. Nollet, J. C. Martins, F. Vanhaecke, A. Vantomme, C. Delerue, G. Allan, and Z. Hens, *Size-Dependent Optical Properties of Colloidal PbS Quantum Dots*, ACS Nano, 3(10), 3023 (2009); <https://doi.org/10.1021/nn900863a>.
- [8] M. Mozafari, F. Mozarzadeh, *Controllable synthesis, characterization and optical properties of colloidal PbS/gelatin core-shell nanocrystals*, Journal of Colloid and Interface Science, 351, 442 (2010); <https://doi.org/10.1016/j.jcis.2010.08.030>.
- [9] M. Scheele, D. Hanifi, D. Zhrebetsky, S. T. Chourou, S. Axnanda, B. J. Rancatore, K. Thorkelsson, T. Xu, Z. Liu, L.-W. Wang, Y. Liu, and A. P. Alivisatos, *PbS Nanoparticles Capped with Tetrathiafulvalenetetracarboxylate: Utilizing Energy Level Alignment for Efficient Carrier Transport*, ACS Nano, 8(3), 2532 (2014); <https://doi.org/10.1021/nn406127s>.
- [10] L. Cheng, Y. Cheng, J. Xu, H. Lin, Y. Wang, *Near-infrared two-photon absorption upconversion of PbS/CdS quantum dots prepared by cation exchange method*, Materials Research Bulletin 140, 111298 (2021); <https://doi.org/10.1016/j.materresbull.2021.111298>.
- [11] A.K. Mishra, S. Saha, *Synthesis and characterization of PbS nanostructures to compare with bulk*, Chalcogenide Letters, 17(3), 147 (2020); <https://doi.org/10.15251/CL.2020.173.147>.
- [12] D.V. Talapin, J.-S. Lee, M.V. Kovalenko and E.V. Shevchenko, *Prospects of Colloidal Nanocrystals for Electronic and Optoelectronic Applications*, Chem. Rev., 110, 389 (2010); <https://doi.org/10.1021/cr900137k>.
- [13] S.V. Kershaw, L. Jing, X. Huang, M. Gao and A.L. Rogach, *Materials aspects of semiconductor nanocrystals for optoelectronic applications*, Mater. Horizons, 4, 155 (2017); <https://doi.org/10.1039/C6MH00469E>.
- [14] M.T. Dieng, B.D. Ngom, P.D. Tall, M. Maaza, *Biosynthesis of Zn₅(CO₃)₂(OH)₆ from Arachis Hypogaea Shell (Peanut Shell) and Its Conversion to ZnO Nanoparticles*, American Journal of Nanomaterials, 7(1), 1 (2019); <https://doi.org/10.12691/ajn-7-1-1>.
- [15] Ankita, S. Kumar, S. Saralch, D. Pathak, *Nanopowder and Thin Films of ZnO by Sol Gel Approach*, J. Nano - Electron. Phys., 11(4), 04027 (2019); [https://doi.org/10.21272/jnep.11\(4\).04027](https://doi.org/10.21272/jnep.11(4).04027).
- [16] O.Z. Didenko, P.E. Strizhak, G.R. Kosmambetova, N.S. Kalchuk, *Synthesis and Morphology of the ZnO/MgO Low-Dimensional Quantum Systems*, Physics and Chemistry of Solid State, 10(1), 106 (2009);
- [17] M. Basak, Md. L. Rahman, Md. F. Ahmed, B. Biswas, N. Sharmin. *The use of X-ray diffraction peak profile analysis to determine the structural parameters of cobalt ferrite nanoparticles using Debye-Scherrer, Williamson-Hall, Halder-Wagner and Size-strain plot: Different precipitating agent approach.* Journal of Alloys and Compounds 895, 162694 (2022); <https://doi.org/10.1016/j.jallcom.2021.162694>.
- [18] A. Guinier, X-ray Diffraction in Crystals, Imperfect Crystals, and Amorphous Bodies. Dover publication incorporation, New York, 1994.
- [19] S. Rajathi, K. Kirubavathi, K. Selvaraju, *Structural, morphological, optical, and photoluminescence properties of nanocrystalline PbS thin films grown by chemical bath deposition*, Arabian Journal of Chemistry 10, 1167 (2017); <https://doi.org/10.1016/j.arabjc.2014.11.057>.
- [20] M. Wati and K. Abraha, *A Study on Fabrication and Structural Characterization of PbS Thin Films*, American Journal of Biochemistry and Biotechnology, 13(4), 208 (2017); <https://doi.org/10.3844/ajbbsp.2017.208.214>.
- [21] N.B. Danilevska, M.V. Moroz, B.D. Nechyporuk, N.E. Novoseletskiy, V.O. Yukhymchuk, *The Influence of Technological Modes on the Physical Properties of Cadmium Sulfide Nanocrystals Derived by the Electrolyte Method*, Journal of Nano- and Electronic Physics, 8(2), 02041 (2016); [https://doi.org/10.21272/jnep.8\(2\).02041](https://doi.org/10.21272/jnep.8(2).02041).
- [22] A.V. Lysytsya, M.V. Moroz, B.D. Nechyporuk, B.P. Rudyk, B.F. Shamsutdinov, *Physical Properties of Zinc Compounds Obtained by Electrolytic Method*, Physics and Chemistry of Solid State, 22(1), 160 (2021); <https://doi.org/10.15330/pcss.22.1.160-167>.
- [23] N.B. Danilevska, M. Moroz, N. Yu. Novoseletskyy, B.D. Nechyporuk, B.P. Rudyk, *The influence of technological modes on the physical properties of zinc oxide nanocrystals derived electrolyte method*, Journal of Physical Studies, 20(3), 3601-1 (2016); <https://doi.org/10.30970/jps.20.3601>.
- [24] V.D. Mote, Y. Purushotham, B.N. Dole, *Williamson-Hall analysis in estimation of lattice strain in nanometer-sized ZnO particles*, Journal of theoretical and applied physics, 6(1), 2251 (2012); <https://doi.org/10.1186/2251-7235-6-6>.
- [25] B. Huntington. *The Elastic Constants of Crystals*. Solid State Physics. 7, 213-351 (1958).

- [26] T. D. Krauss, F.W. Wise, *Raman-scattering study of exciton-phonon coupling in PbS nanocrystals*, Phys. Rev. B, 15(55), 9860 (1997); <https://doi.org/10.1103/PhysRevB.55.9860>.
- [27] P. G. Etchegoin, M. Cardona, R. Lauck, R. J. H. Clark, J. Serrano, and A. H. Romero, *Temperature-dependent Raman scattering of natural and isotopically substituted PbS*, Phys. stat. sol. (b) 245(6), 1125 (2008); <https://doi.org/10.1002/pssb.200743364>.
- [28] A.G. Kontos, V. Likodimos, E. Vassalou, I. Kapogianni, Y.S. Raptis, C. Raptis, P. Falaras, *Nanostructured titania films sensitized by quantum dot chalcogenides*, Nanoscale Research Letters, 6(1), 266 (2011); <https://doi.org/10.1186/1556-276X-6-266>.
- [29] A. Milekhin, L. Sveshnikova, T. Duda, N. Surovtsev, S. Adichtchev, D. R. T. Zahn, *Optical Phonons in Nanoclusters Formed by the Langmuir-Blodgett Technique*, Chinese Journal of Physics, 49(1), 63 (2011);
- [30] J.S. Arunashree, N. P. Suresh, S. Sujesh, K.P. Vaishnav, Vishnu, S. Vishnu, M. Prabhakaran, V.V. Ison and C.O. Sreekala, *Surface Modified Lead Sulphide Quantum Dots for In Vitro Imaging of Breast Cancer Cells Adopting Confocal Raman Spectroscopy*, Int. J. Chem. Sci.: 14(4), 1844 (2016);
- [31] A. V. Baranov, K. V. Bogdanov, E. V. Ushakova, S. A. Cherevko, A. V. Fedorov, and S. Tsharntke, *Comparative Analysis of Raman Spectra of PbS Macro- and Nanocrystals*, Optics and Spectroscopy, 109(2), 268 (2010); <https://doi.org/10.1134/S0030400X10080199>.
- [32] O. Portillo-Moreno, R. Gutierrezerez, M. Chavez Portillo, M.N. Marquez Specia, G. Hernandez-Telleza, M. Lazcano Hernandez, A. Moreno Rodriguez, R. Palomino-Merino, E. Rubio Rosas, *Growth of doped PbS:Co²⁺ nanocrystals by Chemical Bath*, Revista, Mexicana de Fisica, 62, 456 (2016);
- [33] M. Cheraghizade, R. Yousefi, F. Jamali-Sheini, A. Saaedi, *Comparative study of Raman properties of various lead sulfide morphologies*, Majlesi Journal of Telecommunication Devices, 2(1), 163 (2013);
- [34] K. K. Nanda, S. N. Sahu, R. K. Soni and S. Tripathy, *Raman spectroscopy of PbS nanocrystalline semiconductors*, PHYSICAL REVIEW B, 58(23), 15405 (1998); <https://doi.org/10.1103/PhysRevB.58.15405>.
- [35] M. Cortez-valadez, A. Vargas-ortiz, L. Rojas-blanco, H. Arizpe-chavez, M. Flores-Acosta, R. Ramirez-Bon, *Additional Active Raman Modes in α -PbO Nanoplates*, Physica E: Low-dimensional Systems and Nanostructures, 53, 146 (2013); <https://doi.org/10.1016/j.physe.2013.05.006>.
- [36] J. L. Blackburn, H. Chappell, J. M. Luther, A. J. Nozik, J. C. Johnson, *Correlation between Photooxidation and the Appearance of Raman Scattering Bands in Lead Chalcogenide Quantum Dots*, J. Phys. Chem. Lett., 2 (6), 599 (2011); <https://doi.org/10.1021/jz2000326>.

Н.В. Мазур¹, А.В. Лисиця², М.В. Мороз³, Б.Д. Нечипорук², Б.П. Рудик³, В.М. Джаган¹, О.А. Капуш¹, М.Я. Валах¹, В.О. Юхимчук¹

Фізичні властивості нанокристалічного сульфідів свинцю отриманого електролітичним методом

¹ Інститут фізики напівпровідників імені В.Є. Лашкарьова НАН України, м. Київ, Україна
kapush-olga@ukr.net

² Рівненський державний гуманітарний університет, м. Рівне, Україна

³ Національний університет водного господарства і природокористування, Рівне, Україна

⁴ Факультет фізики, Київський національний університет імені Тараса Шевченка, Київ, Україна

Досліджено можливість отримання нанокристалічного сульфідів свинцю електролітичним методом з використанням свинцевих електродів та встановлено вплив температури на процес синтезу. На основі проведених рентгеноструктурних досліджень визначено хімічний та фазовий склад отриманих сполук та розмір нанокристалітів методами Дебая-Шеррера та Вільямсона-Холла, а також визначено параметр елементарної комірки досліджуваних кристалів. Результати рентгеноструктурних досліджень порівнюються з даними, отриманими зі спектрів комбінаційного розсіювання світла цих зразків.

Ключові слова: сульфід свинцю, рентгеноструктурні дослідження, розміри нанокристалів, формула Дебая-Шеррера, метод Вільямсона-Холла, комбінаційне розсіювання світла.